

# Cyclic Voltammetry is Invasive on Microbial Electrosynthesis

Sanne M. de Smit,<sup>[a, b]</sup> Cees J. N. Buisman,<sup>[a]</sup> Johannes H. Bitter,<sup>\*[b]</sup> and David P. B. T. B. Strik<sup>\*[a]</sup>

Cyclic voltammetry (CV) is expected to cause changes in the biocathode composition, especially when using low scan rates. A recent finding stated that CV triggered further biocatalytic activity in microbial electrosynthesis systems (MES), leading to the aim of our study: to investigate the invasiveness of CV on MES. The present study confirms that a CO<sub>2</sub> elongation MES biocathode composition changes during and right after the CV. Oxidation peaks differ over repeated CV-cycles while metal compounds and biomass were released in the biocatholyte.

After CV, the current increased temporarily for up to 20 days and the metal compounds decreased from the biocatholyte solution. Further, the sole short application of open cell voltage was shown to shortly increase the current. Evidently CV affects the studied biocathode, which complicates the use of CV as an analysis technique in MESs. However, the positive effect CV has on biocathode current density may provide methods to boost reactor performance and maintain productivity.

## 1. Introduction

Microbial electrosynthesis (MES) is a promising emerging technique for carbon capture and utilization. MES systems consist of an anode and a cathode, where an oxidation and a reduction reaction occur, respectively. The anode and cathode chamber are in most systems separated by a membrane and filled with electrolyte.<sup>[1]</sup> The electrons resulting from the oxidation reaction are transferred to the cathode where they are used as energy source. The reduction reaction at the cathode is catalyzed by microorganisms, which grow either attached to the cathode as a biofilm or suspended in the catholyte.<sup>[2]</sup>

Various MES processes were developed to reduce CO<sub>2</sub> to methane, alcohols and/or elongated carboxylates up to six carbon-chains.<sup>[2c,3]</sup> The technique is promising due to a broad spectrum of biochemicals as products<sup>[2d,3]</sup> and the low use of water and arable land.<sup>[4]</sup> Additionally, the increasing number of sustainable electrical energy sources make MES a promising alternative method for chemical production. However, since the systems are so multifaceted, many parts of the processes remain black boxes. To get more insights in electron transfer

mechanisms, system resistances, mass transfer or electrocatalysts, a broad spectrum of electrochemical analysis techniques can be used.

In electrochemistry, cyclic voltammetry (CV) is used to study mechanisms, kinetics, and irreversibility of homogeneous reactions,<sup>[5]</sup> electrode kinetics,<sup>[6]</sup> catalyst performance<sup>[7]</sup> and electrode surface composition,<sup>[8]</sup> e.g., metal electrodeposition is investigated by reversibly depositing and removing the compound from the electrode during CV.<sup>[9]</sup> A system with a microbial biofilm can be considered to be more complex compared to an abiotic electrochemical system. The electrochemical reactions that are catalyzed by bacteria include multiple steps and transfer processes, especially when enzymatic catalysts are involved.<sup>[10]</sup> Furthermore, a biofilm contains many charged compounds and a pH gradient<sup>[11]</sup> which both slow down charge transfer across the biofilm. The biofilm composition and productivity change over time as the biofilm develops.<sup>[12]</sup> The electrolyte in bioelectrochemical systems is used as microbial medium and therefore contains multiple compounds, while the electrolytes in electrochemical experiments are often less complex.<sup>[10]</sup> Trace metals from the biotic medium could deposit on the cathode.<sup>[13]</sup> The insights from a CV in a biotic system also differ from those in an abiotic system, biotic CVs are mostly used to indirectly measure biocatalytic activity,<sup>[2b,e-g,10,14]</sup> but also kinetic analysis,<sup>[10]</sup> electron transfer<sup>[15]</sup> and biofilm formation<sup>[16]</sup> can be studied with CV.

CV in bioelectrochemical systems is mostly performed with different settings compared to abiotic systems due to the different characteristics. For example, lower scan rates (1 mV/s) are applied in bioelectrochemical CVs,<sup>[17]</sup> to allow the system to recover as much as possible from the potential change and thus minimize the effect of the capacitive current.<sup>[10]</sup> The disadvantage of this lower scan rate is the longer duration of the CV scan, which can affect the experiment. Ruiz, et al.<sup>[17b]</sup> reported significant changes in the culture medium induced by low scan rate CVs in bioelectrochemical systems. Additional indications for invasive effects of CV were found by Jourdin,

[a] S. M. de Smit, Prof. Dr. C. J. N. Buisman, Assoc. Prof. Dr. D. P. B. T. B. Strik  
Environmental Technology  
Wageningen University and Research  
Axis-Z, Bornse Weilanden 9, 6708 WG Wageningen, The Netherlands  
E-mail: david.strik@wur.nl

[b] S. M. de Smit, Prof. Dr. J. H. Bitter  
Biobased Chemistry and Technology  
Wageningen University and Research  
Axis-Z, Bornse Weilanden 9, 6708 WG Wageningen, The Netherlands  
E-mail: harry.bitter@wur.nl

 Supporting information for this article is available on the WWW under <https://doi.org/10.1002/celc.202100914>

 © 2021 The Authors. ChemElectroChem published by Wiley-VCH GmbH. This is an open access article under the terms of the Creative Commons Attribution Non-Commercial License, which permits use, distribution and reproduction in any medium, provided the original work is properly cited and is not used for commercial purposes.

et al.<sup>[2c]</sup> They operated a bioelectrochemical system in which CO<sub>2</sub> was elongated to fatty acids at current densities up to  $-14 \text{ kA/m}^3$  porous cathode. In some cases, after running a CV on a biocathode experiment, the current increased abruptly with 200% compared to before the CV. It was however not clear whether the biocathode composition changed during and/or after the CV. Jourdin, et al.<sup>[2c]</sup> suggested that CV enhances the current only when a fully developed biofilm is present since the CVs did not affect the current earlier in the same experiment. The mentioned increase of current has applicable relevance, as higher current densities lead to a higher availability of electron donors for (microbial) cathodic reactions. Although it is clear that CV may cause irreversible changes, especially at low scan rates, the effect of CV on the biocathode composition and bioelectrosynthesis system performance has never been studied before.

Therefore, our study objective was to investigate the invasiveness of cyclic voltammetry on the biocathode of a microbial electrosynthesis system.<sup>[2c]</sup> We measured the effect of CV on system performance and biocathode composition during CO<sub>2</sub> elongation to acetate in a system comparable to that of Jourdin, et al.<sup>[2c]</sup> The biotic reactor was inoculated with a mixed culture of microorganisms from various chain elongation processes.<sup>[2c,4,18]</sup>

The effect on system performance is shown by the current response. Between long-term operation and the CV scan, open cell voltage (OCV) was shortly applied to switch the operation mode. Since the OCV goes paired with a change in cathode potential, the effects on current of OCVs as well as some operational difficulties (pH instability, reactor leakage) were investigated. The effect of CV on current was also studied in abiotic systems. Three sets of duplicate abiotic experiments were used to study the effect of a smaller potential range and of a longer application of reducing potentials during CV. Both the biotic and abiotic systems were operated in continuous mode with a 3D carbon felt electrode as used by Jourdin, et al.<sup>[2c]</sup> The effect of CV on the biocathode composition was measured by monitoring the (bio)catholyte metal species elements concentrations (Al, Ba, Co, Cu, Fe, Mg, Mn, Mo, Ni and Zn) and optical density (i.e. biomass concentration) during and after the CV scan.

## 2. Results

To study the invasiveness of CV on a microbial electrosynthesis system, CVs were performed at five different moments during continuous long-term (239 d) operation of a CO<sub>2</sub> elongation system. The biocathode was continuously elongating CO<sub>2</sub> to acetate from day 5 onwards at an HRT of 4 days. The biocathode potential was kept at  $-0.85 \text{ V}$  vs SHE and the bioreactor pH was controlled at  $5.8 \pm 0.1$  (SI Figure S1 and S2). Since Jourdin, et al.<sup>[2c]</sup> suggested that the CV would only have effect with a biofilm present, the CVs were not performed in the biotic reactor until a well-developed by eye visible biofilm was present. The bioreactor was operated for 125 days prior to the first CV scan for the biofilm development (SI Figure S2). The

effects of CV are split in two categories. Firstly, the effect of CV on current and acetate productivity (reactor performance) was measured. Secondly, the effect of CV on the biocathode composition was investigated, e.g., the change of biocatholyte metal species and biomass concentration.

### 2.1. Effect of Cyclic Voltammetry on Reactor Performance

#### 2.1.1. CV Enhanced the Current in a Bioelectrochemical CO<sub>2</sub> Elongation Reactor

The effect of CV on system performance was measured by the change in current. The current is cathodic, so a more negative value corresponds with increased current. The current in the bioelectrochemical CO<sub>2</sub> elongation reactor increased after every performed CV scan.

Directly after the CVs, current increases to approximately 5 times the value before the CVs were observed (Figure 1A and SI Figure S3). These initial current increases lasted short (Figure 1A), but hereafter the current stabilized at more negative values compared to before the CVs. The value at which the current stabilized after this initial peak showed some variation over the various biotic CV scans (Figure 1A, SI Figure S2). The longest current increases occurred after CV1 and CV4, with durations of 75 days and 20 days, respectively, before stabilizing again to the value prior to those CVs.

#### 2.1.2. Current Increase After Biotic CV and Not After Abiotic CV

Three duplicates of abiotic experiments were performed to compare the effects of CV on electrochemical systems without a biofilm or suspended bacteria present. The current graphs in time during abiotic control experiments are shown in the SI Figure S4. The current of the abiotic reactors was higher compared to the current in the biotic reactor prior to the first biotic CV scan. After 8 days of operation, CV scans were run on these abiotic systems. One set of abiotic CVs (reactors I and II) had the same potential range as the biotic CVs ( $-1.41$  to  $-0.21 \text{ V}$ , all vs Ag/AgCl). Since voltage overload occurred at the most negative potential values ( $< -1.2 \text{ V}$ ), smaller potential ranges were used for the other two sets of abiotic experiments to compare the CVs with and without voltage overload. The CVs of abiotic reactors III and IV had a potential range of  $-1.10$  to  $-0.21 \text{ V}$ . The CVs of abiotic reactors V and VI had the same potential range ( $-1.10$  to  $-0.21 \text{ V}$ ) and a potential hold at 620s at potential  $-1.10 \text{ V}$  to simulate the longer exposure of the cathode to negative potentials similar to the experiments with voltage overload.

In contrast with the biotic currents, the abiotic currents didn't increase but stayed unaffected by the CVs. All initial current increases (8 h after the CVs) are shown in Figure 2. To measure the initial current increase after the CVs, 0.34 days (8 h) was depicted as the duration for the short-term increase based on the shape of the current graphs. The average current values calculated over the 5 days before biotic CVs 2 to 5 are

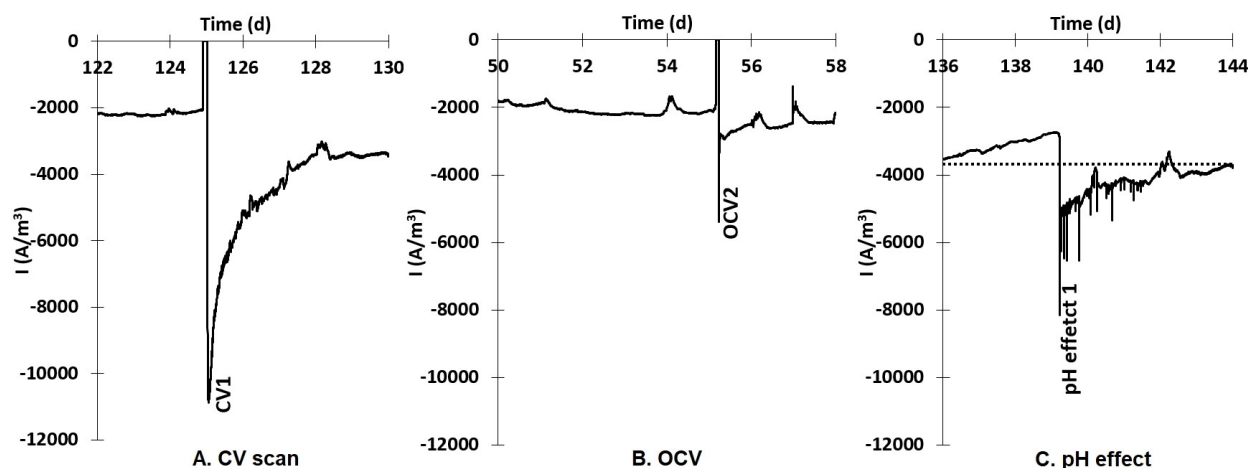


**Figure 1.** Initial and longer (3 to 5 days) term effect of cyclic voltammetry (A), open cell voltage (B) and change of pH (C) on the current in time (per  $\text{m}^3$  cathode) in a bioelectrochemical  $\text{CO}_2$  elongation system. The dotted baseline represents the stabilized current at pH 5.8 (C). At day 136, the pH control was off so the pH increased to 6.5 until day 139, when the pH control was turned on again. The current values during the CV scan are not shown in this graph (A), they can be found in SI Figure S6. The full graph of current in time for this reactor is shown in SI Figure S2.

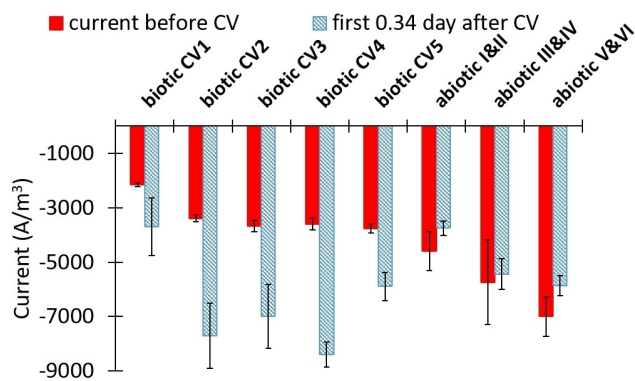


**Figure 2.** Increase in current in the first 8 h after five cyclic voltammetry scans performed on a biotic (CV1–CV5) and the three abiotic duplicates: I and II (CV from  $-0.21$  to  $-1.41$  V), III and IV (CV from  $-0.21$  to  $-1.10$  V) and V and VI (CV from  $-0.21$  to  $-1.10$  V with 620 sec potential hold at  $-1.10$  V) electrochemical  $\text{CO}_2$  elongation system. The error bars show the standard deviations between the different measurements in time (measured every minute).

comparable (Figure 2), showing that the current eventually decreased after the first five days right after biotic CVs 1 to 4.

In the biotic reactor, the current increased not only after CVs, but also after certain operational measures. For example, short current peaks were also observed after moments where open cell voltage (OCV) or temporary pH changes occurred. These effects are discussed in the next section.

### 2.1.3. OCV and HCl Addition Affect the Current Temporarily

As mentioned before, short current peaks were not only observed after biotic CV scans, but also after operational measures with OCV or short pH changes in the biotic system. Open cell voltage (OCV) is shortly applied to switch the operation mode between long-term operation and the CV scan. To study the current responses in more detail, Figure 1 shows

the current of the biotic reactor in the days before and after OCV (B) and a pH issue (C). The current increased (to a more negative value) directly after the OCV. This initial current increase peak is smaller than the initial increase peaks after CV (Figure 1A). Approximately one day after the OCV, the current stabilized at a value similar to the current before the OCV, as shown in more detail in Figure 1B. Over the whole course of the biotic experiment, five OCVs occurred separate from CVs, with durations ranging from 1.5 to 15 hours (see experimental section). After OCV1 to OCV4, the current increased for 19 h, 43 h, 5 min and 53 h for OCV1–4, respectively, before decreasing to the value prior to the OCVs. The current increase after OCV5 lasted longer, as the current did not decrease to the value before OCV5 for 20 days (SI Figure S2).

Another operation issue that influenced the current was a change in the bioreactor pH, as shown in Figure 1C. The current was observed to increase when pH dropped, whereas it decreased when pH rose. For example, when the pH was not controlled and increased from 5.8 to 6.5 by day 139, the current increased directly after the pH controller was turned on again and HCl was added to decrease the pH to 5.8. Four days afterwards, the current stabilized at a value similar to before the pH change (Figure 1C). The current increases after the HCl addition had the same durations as for the OCV; the current increased the current for 44 h, 10 h and 1 h, measured until the current was similar to the current before the pH effect (SI Figure S2). During the CVs, the HCl addition for the pH control did not change compared to the addition during continuous operation (SI Figure S1). Therefore, the effects of CV on the current can't be caused by changes in the bulk catholyte pH.

Leakages of the bioreactor also affected the current. Two leakages occurred during the operation of the biotic system (indicated in SI Figure S2). After the first leakage (day 183) the current increased for 40 minutes, while after the second leakage (day 217) the current increased to twice its value and did not

stabilize at the same value as before the leakage for the remaining 20 days of the experiment.

#### 2.1.4. It Could Not be Revealed Whether Acetate Productivity was Affected by the CV

Besides the current, the effect of the performed CVs on acetate productivity was also studied. The acetate productivity in time is shown in Figure 3. From day 98 to 183 the acetate productivity increased steadily, and no evident direct effect of CV was revealed. To draw conclusions about the effect of CVs on the acetate productivity, steady state performances before and after a CV should be compared. With the hydraulic retention time of 4 days, a steady state period should take approximately 12 days. However, the acetate productivity was never stable for 12 days straight during the performed experiment. Therefore, the bioreactor did not perform stable enough to select steady state periods.

The leakage at day 183 affected not only the current, but also the acetate productivity, as it dropped to  $2.4 \pm 1.9$  mmol C/L/day. Besides the acetate productivity, the electron recovery was also calculated and shown in the SI Figure S5. The electron recovery never reached high numbers (e.g. > 90%) so there

was possibly a surplus of electron supply to the biofilm or suspended bacteria.

#### 2.2. Effect of Cyclic Voltammetry on Biocatholyte Metal Species Elements and Biomass Concentrations

After investigation of the effect of CV on system performance, the effects of CV on the (bio)cathode composition were studied. To keep these measurements the least invasive, the biocatholyte was investigated.

##### 2.2.1. Biomass and Metal Species Increase in Biocatholyte During the CV Scan

During the CV scans in the biotic system, the optical density ( $OD_{600}$ ) increased from  $0.047 \pm 0.011$  to  $0.142 \pm 0.049$  (averaged over the scans on day 147, 174 and 224). Microscopic observations supported that the amount of suspended cells was substantially higher after the first oxidation peak of the CV compared to before the CV (SI Figure S7). The optical density during the CV of the abiotic experiments increased only from  $0.004 \pm 0.000$  to  $0.008 \pm 0.001$  (SI Table S1 and S2).

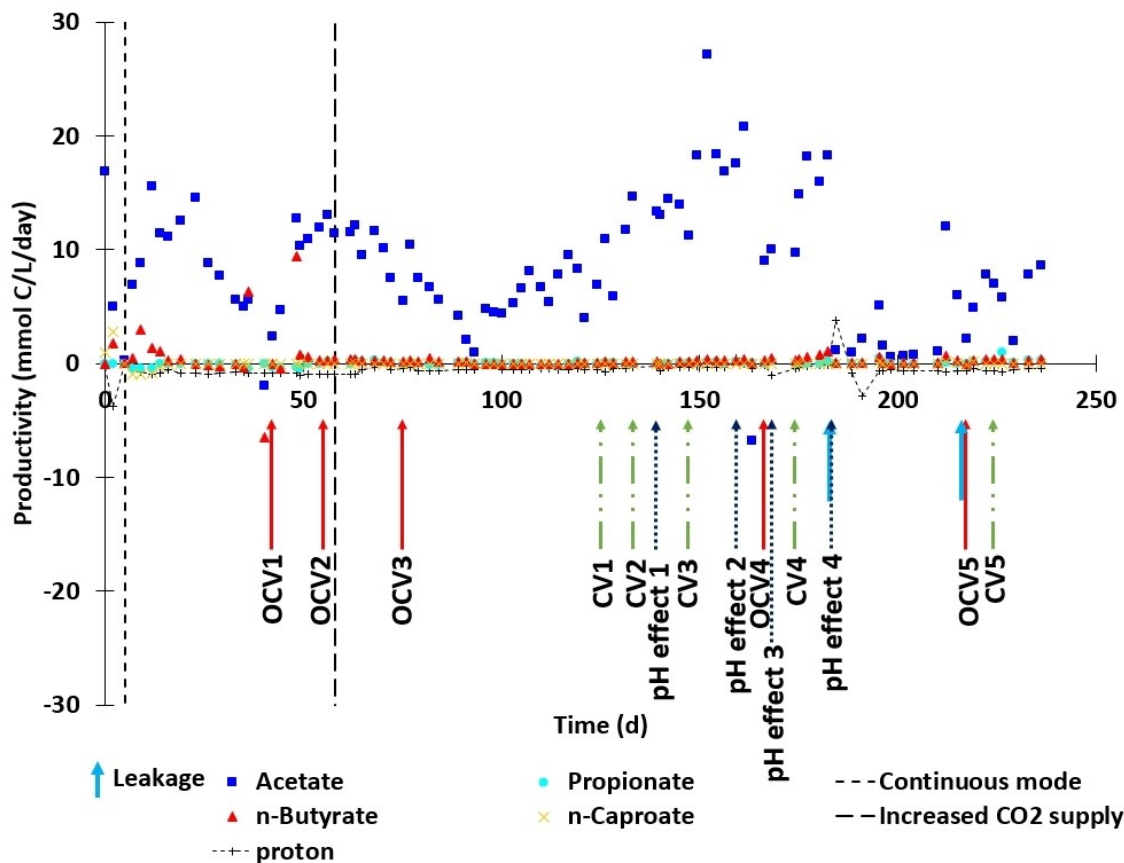


**Figure 3.** Volumetric productivity of acetate, propionate, n-butyrate and n-caproate in time in a bioelectrochemical  $\text{CO}_2$ -fed system. The proton production is shown in  $\text{mmol H}^+/\text{L/day}$ . At day 5, the biotic reactor was put into continuous mode, the  $\text{CO}_2$  supply rate was increased ten-fold at day 58. The CV scans are indicated by long green dash double dotted arrows, the open cell voltage applications are indicated by red arrows and changes in the pH that affected the current are indicated by the blue dashed arrows. The light blue arrows indicate reactor leakages.

In addition to biomass, the concentrations of metal atoms in the biotic catholyte before and after CV 2 to 5 were measured to investigate whether the CV caused net changes in the catholyte metal composition (Figure 4). Possibly the metal atoms were present in the catholyte as ions, complexes and/or as part of enzymes and microbes. The used measuring method gives the element concentrations of the metals, so the exact composition or oxidation state of the released metal species remains to be studied.

The actual catholyte concentrations (including suspended biomass) of iron, aluminium, barium, manganese, and cobalt were significantly higher after the CV scan in the biotic system (Figure 4A). The concentration increase after the biotic CVs is highest for iron and cobalt (346 and 24 times, respectively).

In the abiotic systems, iron cobalt and molybdenum increased in the catholyte, although the concentrations of these compounds in the catholyte after the CV are lower than in the biocatholyte after the CV (Figure 4B). The (bio)catholyte concentrations of all the measured compounds that changed during and after the CV are shown in SI Figure S8, S9 and S10.

Remarkably, the zinc concentration in the biotic reactor catholyte was significantly higher compared to the medium concentrations. Compared to the microbial growth medium, the zinc concentration in the catholyte was approximately 20 times higher in the reactor catholyte after it had been added

to the reactor (see SI Table S3). Leaching tests revealed that zinc leached from reactor parts, especially from the neoprene material used as gasket in the flat plate reactors (SI Table S4). The leaching already occurred before potential was applied to the system which means there is no pure electrochemical behaviour responsible for this zinc release. For the abiotic experiments, that were carried out after the biotic experiment, silicone gaskets were used to prevent zinc leaching.

Since the catholyte zinc concentrations in the biotic and abiotic experiments did not change significantly during the CVs (SI Figure S8, S9 and S10), the zinc leaching was considered negligible. The release of the different metal compounds shown in Figure 4 led to the question whether an electrodeposition or release process could be observed from the shape of the cyclic voltammograms, which will be discussed below.

### 2.2.2. First Cycle of Biotic CV has a Different Oxidation Peak as the Second and Third Cycle

All the performed CV scans consisted of three cycles. The first cycle of the CV scan performed on the bioelectrochemical CO<sub>2</sub> elongation system has a different shape compared to the second and third cycle (Figure 5). The first cycle shows an oxidation peak at a potential around  $-0.5$  V (vs Ag/AgCl), while the second and third cycles have oxidation peaks at a potential around  $-0.62$  V (vs Ag/AgCl) (Figure 5A). The deviation of the first cycle was shown for all five CVs performed on the biotic reactor (SI Figure S6). The second cycle was identical to the third for all five biotic CV scans (Figure 5 and SI Figure S6).

For all reduction waves, potentials more negative than  $-1.1$  V vs Ag/AgCl could not be reached (Figure 5A and B). The maximum voltage between anode and cathode (10 V) was not sufficient to achieve these desired cathode potentials. Two sets of duplicate abiotic CV experiments were carried out to study CVs without this voltage overload (Figure 5C and D). The CV of the first set was performed with a potential range of  $-0.21$  to  $-1.1$  V vs Ag/AgCl (Figure 5C and SI Figure S11B). During the voltage overload in Figure 5B, the cathode was under reducing conditions and high current in the potential range of  $\sim 1.2$  to  $-1.41$  V. To recreate this in a similar but controlled way, in the second set the potential was held at  $-1.1$  V vs Ag/AgCl for 620 sec (Figure 5D and SI Figure S11C).

The different cycles of both the biotic and abiotic CVs have reduction peaks (potentials below  $-0.7$  V vs Ag/AgCl) with different shapes for the different cycles. Remarkably, in all voltammograms, the forward scan (negative to positive) shows more negative current compared to the reverse scan for the reduction peaks. This illustrates that the voltage overload didn't affect the scan cycle direction.

Since the oxidation peak of the first cycle had a different potential compared to those from the second and third cycle, the metal composition of the biocathode could also change differently in the first cycle compared to the second and third cycle. To study the metal composition, multiple catholyte samples were taken in time during the CV.

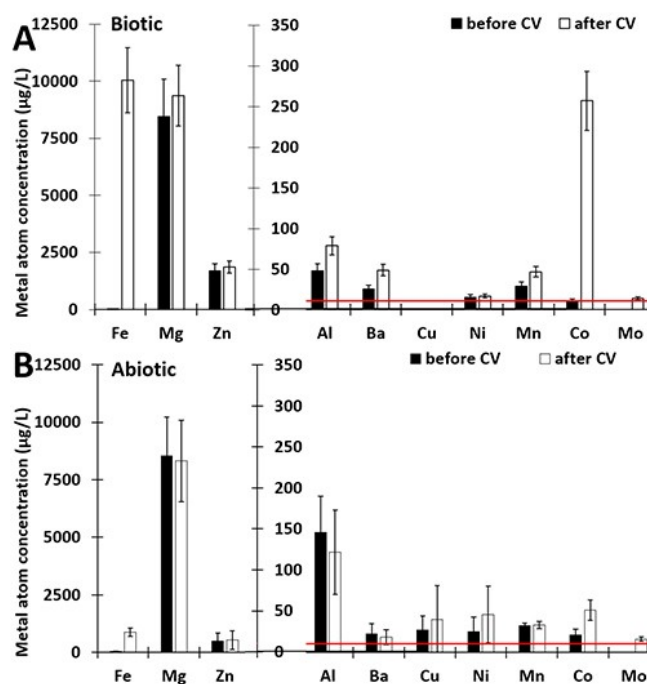


**Figure 4.** Catholyte concentrations of various metal atoms in the biotic (A) and abiotic (B) electrochemical CO<sub>2</sub>-fed reactors before and after the CV treatments. Fe, Mn, Co and Mo were measured before and after CV2-CV5, while Mg, Al, B and Ba were only measured before and after CV5 of the biotic system. The standard deviations (error bars) of the biotic metal atom concentrations were calculated from the average relative standard deviation for Fe, Mn, Co and Ni measured before and after CV2-5 (A). The error bars for the abiotic experiments indicate the relative standard deviation between the six different reactors (B). The red line shows the detection limit of the metal atom concentrations.

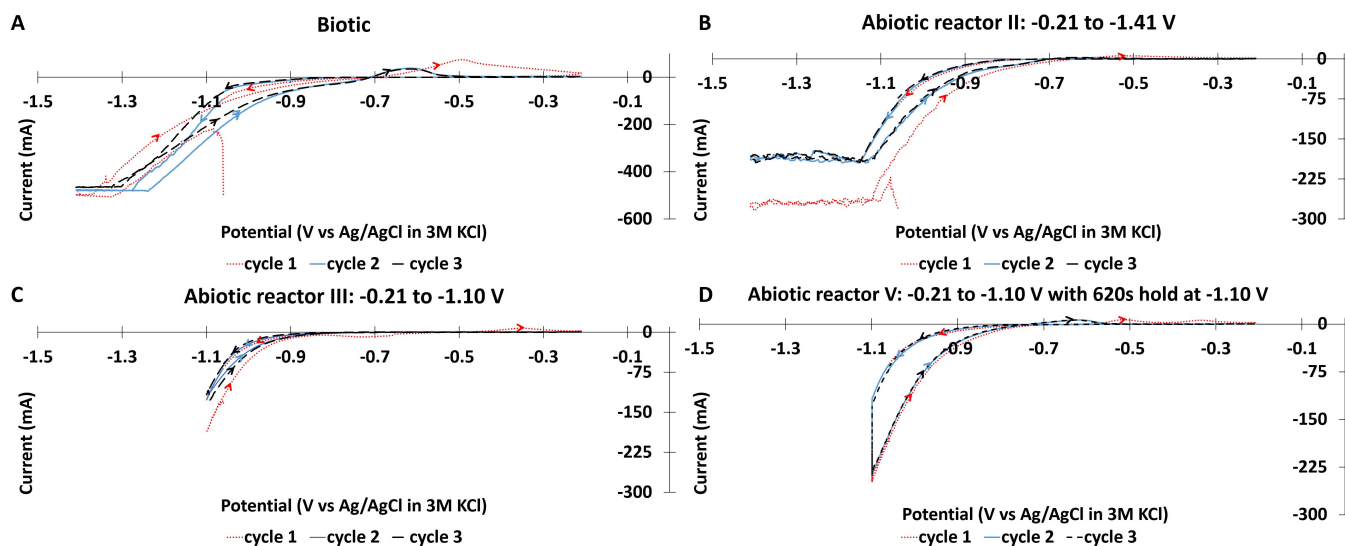


**Figure 5.** Cyclic voltammograms run with the bioelectrochemical CO<sub>2</sub> elongation reactor (A: day 224) and the abiotic systems (B: II) with start potential  $-1.06$  V, the lowest potential  $-1.41$  and the highest potential  $-0.21$  V (all vs Ag/AgCl), the CVs contained three cycles. Potential values more negative than  $-1.2$  V for the biotic scan (A) and more negative than  $-1.1$  V for the abiotic scan (B) could not be reached as a voltage overload occurred. Therefore, two more sets of abiotic experiments were run. The CVs of these experiments had a potential range from  $-0.21$  to  $-1.10$  V (C and D). For the experiments shown in Figure 4D, the potential was held at  $-1.10$  V for 620 sec during each cycle. The scanning direction is indicated by arrow heads. The cyclic voltammograms for the duplicate abiotic experiments are shown in SI Figure S11.

### 2.2.3. Increase of Biomass and Metal Species in Catholyte Mainly Occurred Simultaneous with First Oxidation Peak

Biocatholyte samples were taken at different moments during the CVs to elucidate when the increase in biomass and metal species occurred. The major increase of iron, cobalt, manganese, and molybdenum in the biocatholyte occurred simultaneous with the oxidation peak of the first cycle of the CV scan for both the biotic CVs (after 1550 min) (Figure 6A and SI Figure S8). The biocatholyte concentrations of these metal atoms decreased simultaneous with the subsequent reductive current in the reverse scan (positive to negative, from time 2000–2750 s) and increased simultaneous with the oxidation peaks. Still, the increase was less compared to the first oxidation peak (Figure 6A).

Aluminium, barium and magnesium show different trends. The biocatholyte concentrations of aluminium and barium increased when the CV was at low potentials and the magnesium catholyte concentration increased gradually during the complete biotic CV scans (SI Figure S8A and C). The biocatholyte OD<sub>600</sub> in the biotic system also increased simultaneous with the first oxidation peak of the CV and much less with the potential values of the reduction peak (Figure 6A). One test was performed to gain preliminary insights on the form (precipitated and/or more dissolved) of the metal species that increased in the catholyte, and whether the metal species could be attached to the bacteria. For this test, the centrifuged biomass/solids pellet was separated from the supernatant and separately analysed. The sample used for this experiment was taken 1550 s into the CV, so after the biggest increase of both biomass and metal compounds in the biocatholyte, performed at day 224. Only measurable amounts of iron, zinc, sulphur and

phosphorous were found in the pellet. The concentrations of cobalt, iron, magnesium, and zinc were lower in the supernatant sample compared to the non-centrifuged original sample (SI Table S5).

The abiotic systems showed similar trends compared to the biotic systems. The iron, cobalt, molybdenum, and nickel catholyte concentrations increased also mainly simultaneous with the oxidation peak of the first CV cycle (after 1550 min) (Figure 6C, E and G). The concentrations of aluminium, barium and magnesium did not change significantly during the abiotic CVs, in contrast to the biotic CVs (SI Figure S9A and C, S10A, C, E and G). Remarkably, the current kept increasing although the potential was kept constant in the abiotic experiments with a potential hold at  $-1.10$  vs Ag/AgCl for 620 sec (Figure 6G time 2400–3000 and 4800–5400).

After the CV scan on the biotic cell, the biocatholyte concentrations of most released metal species (iron, cobalt, manganese, molybdenum) decreased during the initial current increase, with the trend similar to the iron shown in Figure 6B (SI Figure S8B and D). Aluminium and barium take longer to reach the concentrations similar to before the CV in the biotic experiment, while they remain unchanged during the abiotic experiments. Their trends were similar to the magnesium shown in Figure 6B (SI Figure S8B and D). All metal atoms that significantly increased in the catholyte during the CVs of the abiotic experiments (iron, cobalt, molybdenum, and nickel), decreased rapidly simultaneous with the initial current peak after the CVs as well (Figure 6D, F and H and SI Figure S9B and D and S10B, D, F and H).

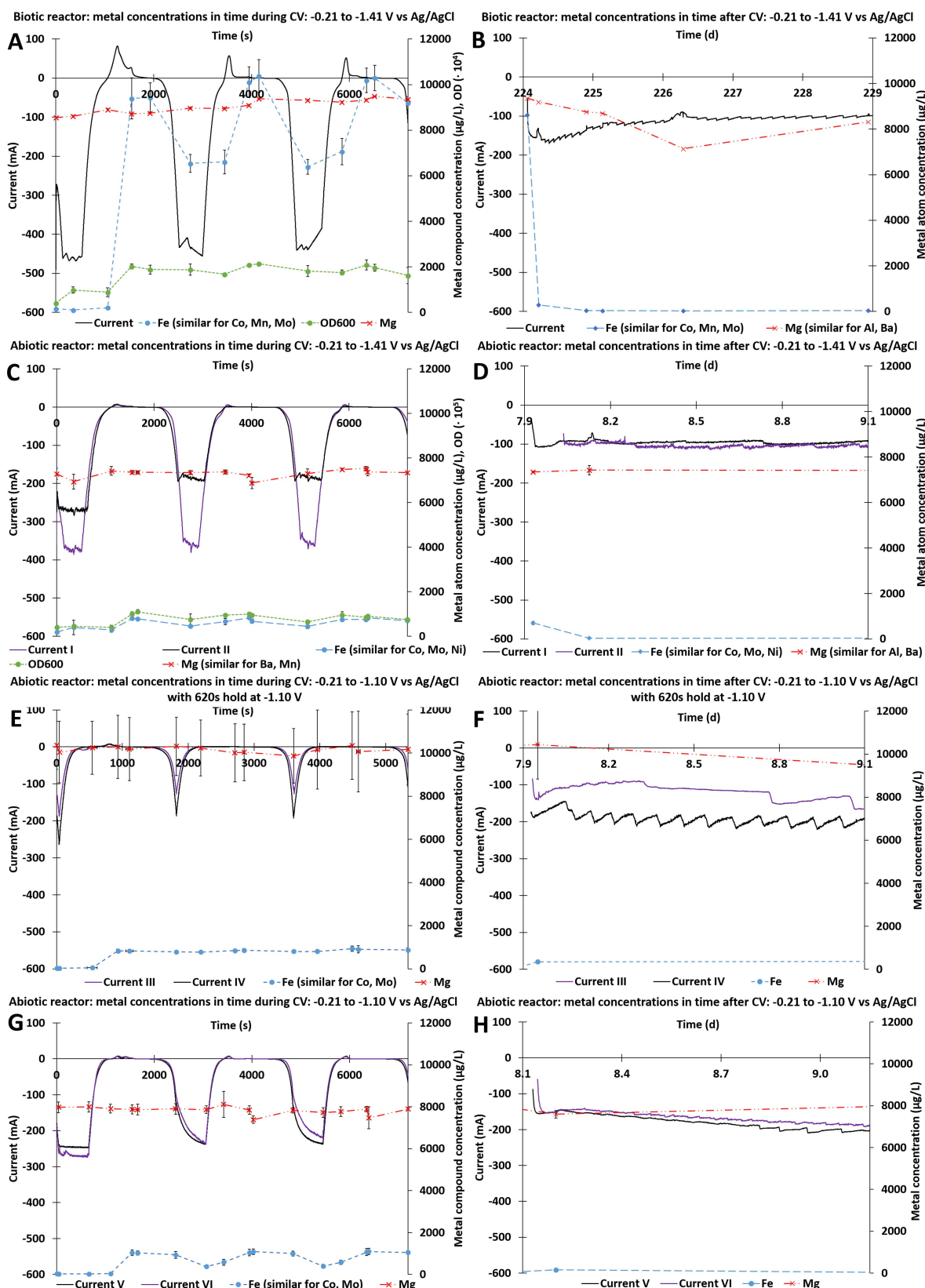


**Figure 6.** Change in concentrations of metals and the optical density ( $\text{OD}_{600}$ ) of the catholyte in time with the change in current during the 3 cyclic voltammetry (CV) scan performed on day 174 (CV4) and day 224 (CV5) with the bioelectrochemical  $\text{CO}_2$  elongation system (A) and during the CV scan performed with the three abiotic duplicates: I and II (CV from  $-0.21$  to  $-1.41$  V; C), III and IV (CV from  $-0.21$  to  $-1.10$  V; E) and V and VI (CV from  $-0.21$  to  $-1.10$  V with 620 sec potential hold at  $-1.10$  V; G). The change in current and the catholyte iron and magnesium concentrations in time after the CV scan performed on day 224 (CV5) with the bioelectrochemical  $\text{CO}_2$  elongation reactor (B) and after the CV performed with abiotic reactors are shown as well: I and II (D), III and IV (F) and V and VI (H). The vertical error bars indicate the minimum and maximum values found during the CV scans on the different days (A) and the difference between the duplicate experiments (C–H), the horizontal error bars indicate the different sampling moments during the different CV scans (A, C, E and G). The arrows indicate the axes used for the different graphs. The potential was controlled on  $-0.85$  vs SHE after the CVs (B, D, F and H).

### 3. Discussion

#### 3.1. CV is Invasive on Microbial Electrosynthesis

Since the first cycle of the biotic CVs is different from the second and third (Figure 5), one can already state that the first cycle is changing the CV response of the biocathode and as such is invasive on the electrochemical CV response. The change of biotic CV scan profile after the first cycle indicates that an oxidation reaction occurs during the first cycle, which then does not occur during the second and third cycle. Three additional findings showing the invasiveness of the CVs are the changed metal compound concentrations in the biocatholyte after the CVs (Figure 4), the increased optical density (Figure 6A) and the increased current directly after the CVs (Figure 1A). The invasiveness is shown to be reproducible as well, as the biotic CV graphs and corresponding metal species behaviours were similar for the five different CVs.

#### 3.2. Increase of Metal Compounds in Biocatholyte can be Related to Metal Oxidation

The metal compounds mainly increased simultaneous with the oxidation peak of the first cycle (Figure 6A), so the changed metal concentrations in the biocatholyte after the CV scan seem related to the different oxidation peak in the first CV cycle. As will be discussed in more detail, the metal atom measurements can represent various forms of metal containing compounds. These compounds originate from the microbial medium or from grown, metal-containing micro-organisms. Measurements in the anolyte showed no detectable metals (data not shown). Thus, the increase of the metal compounds in the catholyte was likely due to their release from the biocathode, as that was the most evident source of released metal atoms and biomass. The initial concentrations of metals present in the catholyte were lower compared to the medium concentrations, indicating accumulation of metals on the biocathode during operation prior to the CV scan.

Although only the element concentrations were measured in this study, we wanted to theoretically predict the speciation of different trace metals during the change of potential. To this end, Pourbaix diagrams were calculated from the catholyte medium concentrations, they are shown in SI Figure S12. The potential and pH area covered by the CV is indicated by red arrows in these diagrams. The potential range of the CV theoretically allows reduction and oxidation of most trace metals in the used medium; cobalt, copper, iron, molybdenum, nickel, and zinc are predicted to change oxidation state from a suspended to a solid form within the potential range of the CVs (SI Table S6 and Figure S12). The behaviour of manganese, copper, and nickel cannot be explained based on purely their Pourbaix diagram. Manganese is released while the oxidation state theoretically does not change (SI Figure S12M and N) and copper and nickel are not released while their oxidation states changes from solid to suspended during oxidation according to the Pourbaix diagrams (SI Figure S12G, H, Q and R).

Assuming that the metal compound oxidation state change into a solid form corresponds to deposition, the Pourbaix diagrams support that the release and deposition of metals is an electrochemical process.<sup>[9a,19]</sup> For example, metal species could be reduced to their solid form and thereby electro-deposited at the cathode during the reduction of the CV and oxidized to their suspended form and electro-released from the cathode during the oxidation of the CV (Figure 7A). The oxidation reaction likely caused their release from the cathode during CV for cobalt iron and molybdenum which predominantly increased in the biocatholyte simultaneous with the first oxidation peak. During the reductive part of the reverse scan (positive to negative), part of the metals is re-electrodeposited, as the catholyte concentrations decreased again (Figure 6). The reductive part of the reverse scan has lower current compared to the reductive part of the forward scan, which is unusual.<sup>[5]</sup> To test whether these directions were caused by the voltage overload, the current behaviour was compared to the abiotic scans without voltage overload. The current behaviour of the abiotic CVs with the voltage overload is similar to the CVs with the “potential hold”. Therefore, the voltage overload was not the reason for the scan directions during the reduction peak. The higher current in the forward scan could be explained by electrodeposition during the reverse scan,<sup>[19–20]</sup> hereby forming a catalyst. Many of the microbial trace metals could be part of a hydrogen evolution catalyst (Mn, Ni, Co, Cu, Fe, Mo).<sup>[21]</sup> This catalyst can decrease the overpotential of e.g. hydrogen evolution, thus causing the increased current in the reductive part of the forward scan.

The catholyte metal concentrations at the end of the CV are still higher than before the CV, indicating different chemical conditions before and after the CV. An explanation for the different metal conditions after the CV could be kinetic hindrance of metal deposition and nucleation. In the abiotic scans that had a “potential hold” at  $-1.10$  V, the current eventually reached values similar to the first reduction peak (Figure 6C), while this was not the case in the scans without this hold (Figure 6A). The current increase during the moments where the potential was held constant at  $-1.10$  V indicates that equilibrium was not yet reached. Apart from the current, the metal catholyte concentrations of iron and molybdenum also change during the “potential hold”. This could indicate capacitive current or deposition of metal species on the cathode. After the CV scans, the applied reducing potential ( $-1.06$  V) allowed enough time for the remaining dissolved metal species to redeposit on the cathode or re-enter the electrical double layer, while a part of the released metal species is washed out due to the continuous operation. Iron, cobalt, manganese, and molybdenum decreased rapidly from the biocatholyte after the CVs, suggesting that these compounds were electrodeposited at the cathode under the reductive conditions.

Investigating the involved deposition mechanisms can help understand the current behaviour after the CV. Remarkably, the current was high at the moments where the metals were released from the biocathode. The supporting information contains an extensive hypothetical framework further linking

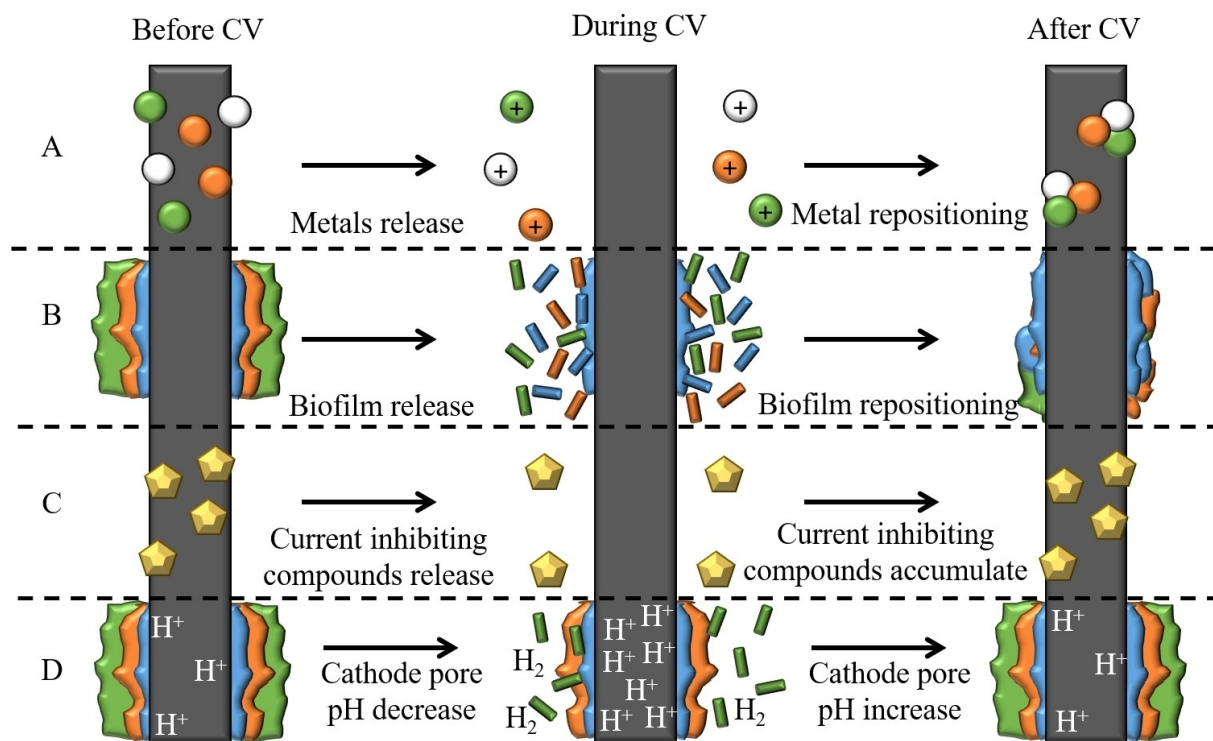


**Figure 7.** Schematic representation of possible processes that are induced by Cyclic Voltammetry in a bioelectrochemical system. CV induces release of metals (A), biofilm (B) and/or current inhibiting compounds (C) that deposited on the cathode over time. A fourth hypothesis is a CV-induced pH decrease inside the cathode (D). After CV, the released compounds are deposited back on the cathode. The metals (A) and biomass (B) is redeposited in a different configuration.

the metal behaviour and the current response. by explaining 4 hypotheses: I) cofactor replacement, II) metal rearrangement, III) biomass thickness decrease and IV) release of dead bacteria (Figure S13). Possible ways for more in-depth research of the metal behaviour include performing the CV with various scanning rates and a study of the cathode surface.

### 3.3. Metal Release Possibly due to Attachment to Biomass

The increase of optical density and most presumably biomass after the biotic CVs raised the question whether the released metals were attached to or part of the biomass that was released from the cathode. Metals are continuously supplied via the microbial growth medium. The metals can be used as cofactor for chain elongation enzymes<sup>[22]</sup> or electron transport mediators. Furthermore, it is known that metal species can attach to bacteria by the chelating properties of the bacterial membranes or by nanoparticle formation.<sup>[23]</sup> It should be noted that the biomass was not fully destructed before performing ICP. This could be done by digestion of the samples but was not performed to prevent dilution of the samples. Thus, the metals attached to the not fully degraded biomass might not have been detected in this study and the actual concentrations of metal compounds in the measured samples might be higher than shown in this study. The measurement of the separated pellet and supernatant indicates that metals were not solely

present in the supernatant but also attached to precipitants and/or part of the biomass. Therefore, (parts of the) iron and zinc could have been incorporated in parts of the biofilm that was released during the CV. The reason why the biomass was released will be discussed in the next section.

### 3.4. Biomass Release Probably Due to Oxidative Current

Remarkably, the major biomass release did not occur when visible bubbles are formed at the cathode during hydrogen evolution (potentials more negative than  $-0.56$  V vs Ag/AgCl, calculated as described by Sleutel<sup>[24]</sup> for our conditions), but simultaneous with the oxidation peak of the CV scans. A possible explanation for this phenomenon is the change of surface charge. When bacteria form a biofilm on a charged surface, it is likely that the biofilm components, e.g. extracellular polymeric substances (EPS), metal (ions), proteins in the bacterial cell walls, are adapted to the surface charge.<sup>[25]</sup> This surface charge depends on the cathodic current, when the current is negative, the surface will be negatively charged but when the current reaches positive values, the surface will be positively charged. This change of charge could disturb the electrostatic interactions between the cathode and the biofilm and consequently detach and release biomass (Figure 7B). The effect of the biomass release on the system performance should

be investigated in a separate study where the biofilm thickness is reduced (e.g. mechanically) with alternative methods.

### 3.5. Current After CV's Initial Increasing and on Longer Term Decreasing

The current increase after the biotic CVs can be split into different phases. During the first 8 hours after the CV an initial current increase is observed and after that, the current slowly decreases back to the value similar to before the CV scan. The initial peak (peak surface equals  $\pm 3320$  Coulomb) is bigger than the amount of current that would be needed to reduce the released metals ( $\pm 56$  Coulomb), presumably hydrogen formation took place during the initial current increase. As mentioned before, the effect of this additional energy availability on the biofilm performance could not be depicted from this study, since the acetate productivity was only monitored three times per week and no clear steady states on acetate productivity were gained.

The second phase, the slow decrease of the current starting 8 hours after the CVs, showed different patterns for the five different biotic CV scans. This erratic behaviour can have multiple reasons. Firstly, the biofilm develops over time, hereby the biofilm composition can change, and thereby affect the electron transfer in the biofilm. Secondly, operation difficulties could possibly have had additional effects on the current, since the duration of the current increase after the CV in our study also differed from the study of Jourdin, et al.,<sup>[2c]</sup> while the setup was the same. For example, the reactor leakage in the current study that occurred nine days after CV4 could have affected the current apart from CV4 itself, resulting in the longer duration of the increased current. Due to the non-systematic timing between the different CVs a relation between the current response of the CV and the development of the biofilm over time could not be determined. Especially the first CV caused a long current increase (75 d), but the metal species concentrations were not measured after CV1, so no insights could be obtained on the metal behaviour.

### 3.6. OCV and Temporary pH Change Affect the Current as Well

Apart from CV, the current was also affected by OCV and temporary pH changes. The current initially increased when OCV occurred (Figure 1). Therefore, studying the metal concentrations in the catholyte before and after OCV would be interesting to test the invasiveness of OCV.

During the effects of temporary pH changes, the current increased always when the pH decreased. A lower pH makes more  $\text{H}_3\text{O}^+$  ions available for the reduction to hydrogen,<sup>[26]</sup> a small change in pH can cause a big change in hydrogen productivity.<sup>[21]</sup> Another plausible reason for the effect of the pH change on the current could be that the electrostatic interactions of polymers in the EPS change<sup>[27]</sup> in such a way that the electron transport through the biofilm is potentially

enhanced at lower pH. The observed pH effects support a fourth hypothesis, that the local pH on the cathode decreased as a result of the changes in the cathode composition (metals and biomass) (Figure 7D). The lower pH causes a current peak that lasts until the cathode composition and thus local pH is fully restored to the value prior to the CV. Local pH measurements in the cathode during and after CV could further elucidate this hypothesis.

### 3.7. No Current Increase After Abiotic CV Possibly due to Shorter Operation or Absence of Biofilm

The long term ( $>1$  day) invasiveness of the CVs in a biotic system was not found for the abiotic systems, although cobalt, iron, molybdenum, and nickel were also net released into the catholyte after the abiotic CVs (Figure 4). A main difference between the abiotic and the biotic experiments was the cathode composition. The biotic system was running for 125 days prior to the first CV scan, while the abiotic CVs were performed after 8 days to prevent microbial growth in the reactors. During the 125 days in the biotic reactor, a by eye visible biofilm was formed and more metals were net supplied to the system via the continuously added medium. The continuous supply could have caused more electrodeposition of metal compounds on the cathode. The release of accumulated metals on the cathode could be more or different, inducing current enhancing mechanisms. Another electrochemical process that could have caused the current increase after the CVs is the release of current inhibiting compounds from the cathode. For example, calcium phosphate<sup>[28]</sup> and calcium carbonate<sup>[29]</sup> have shown to form current inhibiting precipitates in biocathodes and could have slowly accumulated on the biocathode due to long-term operation (Figure 7C). The slow decrease of the current starting 8 hours after the CVs could then be caused by slow precipitation of current inhibiting compounds.

In the study by Jourdin, et al.,<sup>[2c]</sup> the current stayed high for the 160 days after the current increase directly after the CV scan. The current study shows a more short-term current increase in the biotic reactor (Figure 2). This difference in CV effect is remarkable since the conditions in both biotic  $\text{CO}_2$  reduction experiments were similar. The results from our study suggest that, although the CV scan has invasive effects, the long-term increase in current and productivity observed by Jourdin are not (completely) caused by the CV scan. This difference could also be caused by the thicker biofilm in the study from Jourdin, during which also butyrate and caproate were produced, indicating that the biofilm could have been more developed. Elucidating the mechanisms behind the current increase after the biotic CV can provide tools for improving the system performance of bioelectrochemical systems. Thus, further research on the involved mechanism(s) causing the observed CV effects can reveal how CV could be used as biocathode booster or way to provide maintenance and remove pollutants from the electrode.

## 4. Conclusions

Cyclic voltammetry (CV) is invasive on the investigated microbial electrosynthesis system. CV affects both the reactor performance as well as the biocathode composition. The effect on reactor performance was shown as a current increase after the CV lasting up to 20 days. The effect on the biocathode composition is shown by the change in oxidation peak and release of metals and microbial biomass into the biocatholyte. Various underlying mechanisms may play a role on how CV caused invasiveness. The invasiveness is less shown for the abiotic system since the abiotic control experiments showed no current increase after the CVs and little metal release. The difference with the biotic experiment could be due to the shorter operation time of the abiotic experiments and/or to the absence of a developed biofilm. Evidently, CV is not solely an analysis technique. Further elucidation of the described CV effects may be useful for maintenance or boost biocathode performance.

## Experimental Section

### Reactor Setup and Experimental Conditions

Seven continuous electrochemical cells built in the same way as by Jourdin, et al.<sup>[2c]</sup> were used for this study. One reactor was used for the biotic experiment and six reactors were used as three duplicate abiotic reactors. The cathodes were made from carbon felt. The carbon felt was prepared by leaving it overnight in 1 M HCl, subsequently overnight in 1 M NaOH and finally overnight in demi water. Three layers of carbon felt were used, the size of the cathodes was 25.9 cm<sup>3</sup>. The carbon felt layers were held together

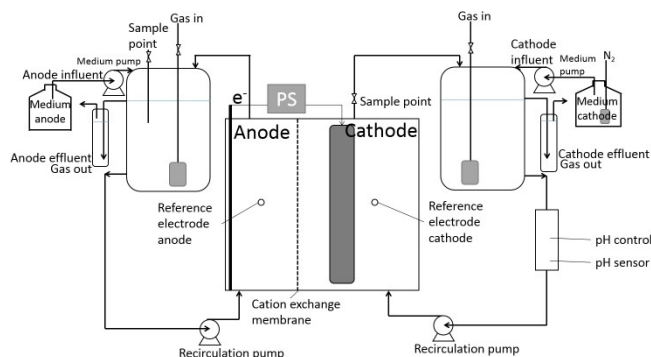


Figure 8. Schematic overview of the (bio)electrochemical cell setup.

by a titanium wire (grade 2) with 0.8 mm thickness, this wire was also used as current collector. The total volumes of the catholyte and anolyte were 345–442 ml and 301–351 ml, respectively including the recirculation tubing (Figure 8). The liquids from the catholyte and anolyte were recirculated at 12 L/h and 10 L/h, respectively. The catholyte recirculation rate was increased from 8 to 12 L/h on day 107 for the biotic reactor.

The pH of the catholyte was controlled at 5.8 with addition of 1 M HCl and 1 M NaOH by a pH controller (Ontwikkelwerkplaats, Elektronica ATV, the Netherlands). The reactor potential was controlled at  $-0.85$  vs SHE with the same potentiostat and reference electrodes (in 3 M KCl) as used by Jourdin, et al.<sup>[2c]</sup> The current was measured every minute with the Ivium potentiostat as done by Jourdin, et al.<sup>[2c]</sup> The reactors were situated in a cabinet in which the temperature was controlled at 30 °C.

The samples were not taken with a needle but from a plastic sample port to prevent external addition of metals into the system.

For the same reason, contact with metal sources was also avoided for all medium stocks and supplies. The sample port was placed directly after the cathode chamber in the recirculation to ensure the samples represented the catholyte next to the cathode.

The biotic reactor was run for 237 days and the abiotic experiments were run for 12 days (Table 1). The biotic reactor was inoculated with mixed culture consortiums from various chain elongation reactors on day 0, 98 and 112. The abiotic experiments were run for a shorter time to prevent microbial growth. The biotic reactor had neoprene gaskets, while the six abiotic reactors had silicone gaskets. CO<sub>2</sub> and N<sub>2</sub> were supplied via a gas sparger (spargerhead was 22 mm height and 12 mm diameter) in the catholyte recirculation bottle at 10 and 23.3 LN/d, respectively for the first phases of the biotic (58 days) experiment. During the second phase of the biotic and during the whole abiotic experiments, the catholyte gas supply was 100 LN CO<sub>2</sub>/d and 233.3 LN N<sub>2</sub>/d. The gas was led through a bottle filled with demi water to humidify the gas before flushing it into the reactor. The CO<sub>2</sub> formed the carbon source for chain elongation during the biotic experiments. The anolyte recirculation bottle was flushed with N<sub>2</sub> to flush away the formed O<sub>2</sub>.

The standard catholyte medium was equal to the medium used by Jourdin, et al.<sup>[2c]</sup> and consisted of (added in this order) 3.17 g/L, sodium 2-bromoethanesulfonic acid, 7.5 g/L Na<sub>2</sub>HPO<sub>4</sub>·2H<sub>2</sub>O, 3.0 g/L KH<sub>2</sub>PO<sub>4</sub>, 0.2 g/L NH<sub>4</sub>Cl, 0.04 g/L MgCl<sub>2</sub>·6H<sub>2</sub>O, 0.02 g/L CaCl<sub>2</sub>·2H<sub>2</sub>O and 1 ml/L trace element solution. NH<sub>4</sub>Cl was left out of the abiotic media to prevent microbial growth. The trace elements used both in this study and by Jourdin, et al.<sup>[2c]</sup> consisted of (added in this order) 1.5 g/L FeCl<sub>3</sub>·6H<sub>2</sub>O, 0.15 g/L H<sub>3</sub>BO<sub>3</sub>, 0.03 g/L CuSO<sub>4</sub>·5H<sub>2</sub>O, 0.18 g/L KI, 0.12 g/L MnCl<sub>2</sub>·4H<sub>2</sub>O, 0.06 g/L Na<sub>2</sub>MoO<sub>4</sub>·2H<sub>2</sub>O, 0.075 g/L ZnSO<sub>4</sub>·H<sub>2</sub>O, 0.15 g/L CoCl<sub>2</sub>·6H<sub>2</sub>O, 0.023 g/L NiCl<sub>2</sub>·6H<sub>2</sub>O and 10 g/L EDTA (C<sub>10</sub>H<sub>14</sub>N<sub>2</sub>Na<sub>2</sub>O<sub>8</sub>·2H<sub>2</sub>O, CAS 6381-92-6). After addition of the EDTA, 7 ml 3 M NaOH was added to the trace element solution to

Table 1. Overview of cyclic voltammetry, open cell voltage and pH effects performed with or occurred to the biotic reactor and the duplicate sets of abiotic reactors.

	Biotic reactor					Abiotic reactors
Total run time	237					12
Cyclic Voltammetry	CV1	CV2	CV3	CV4	CV5	Abiotic CV
Day CV	125	133	147	174	224	8
Open Cell Voltage	OCV1	OCV2	OCV3	OCV4	OCV5	
Day OCV	42	55	75	166	217	
Duration OCV (min)	180	95	119	941	109	
pH effect	1	2	3	4		
Day pH effect	139	159	168	183		

allow dissolving of the metal salts. The pH of the medium was adjusted to 5.8 using 1 M HCl. The anolyte medium was similar to the catholyte medium but did not contain the 2-bromoethanesulfonic acid and no trace elements. Further experiment conditions are all equal to the conditions described by Jourdin, et al.<sup>[2c]</sup> During the continuous biotic experiment, the catholyte and anolyte medium were added with a rate of 3.6 and 3 ml/h respectively to reach a hydraulic retention time (HRT) of 4 days. The duplicate sets of abiotic reactors were run continuous (HRT 4 d) with abiotic medium to simulate the biotic starting conditions.

The effect of CV on a developed biofilm was investigated by performing CV on a continuous bioelectrochemical CO<sub>2</sub> elongation reactor that was running for 125 days. Five CV scans with each three cycles were performed on day 125, 133, 147, 174 and 224 (Table 1). One cyclic voltammetry scan with three cycles was performed on all abiotic reactors at day 8. When performing the cyclic voltammetry (CV), the bioelectrochemical cell was operated at open cell voltage (OCV) 1 minute prior to the CV. OCV also occurred five times during the continuous reactor operation separate from the CVs for 180 min, 95 min, 119 min, 941 min and 109 min on days 42, 55, 75, 166 and 217, respectively (Table 1). As for the CV itself, the start potential was  $-1.06$  V, the potential range was from  $-1.41$  V to  $-0.21$  V for the biotic reactor and abiotic reactors I and II (all vs Ag/AgCl 3 M KCl). For abiotic reactor III, IV, V and VI the potential range was  $-0.21$  to  $-1.10$  V to prevent voltage overload. In the CVs of reactor V and VI, the potential was held at  $-1.10$  V for 620 sec during the CV to allow a similar time under reducing conditions as for the CVs performed in abiotic reactors I and II. The scan rate and potential step were both 1 mV/s and 3 repetitive cycles were performed. Directly after the CV the continuous operation was proceeded (at  $-1.06$  V vs Ag/AgCl) without OCV. For biotic CV4 and CV5 and the CVs in all abiotic reactors, the catholyte was sampled during the CV scans as well. These samples were taken at the start ( $t=0$  sec) and end ( $t=120$  sec) and at the highest ( $-0.21$  V vs Ag/AgCl) ( $t=1550, 3950$  and  $6350$  sec) and lowest potential ( $-1.41$  V vs Ag/AgCl) ( $t=350, 2750$  and  $5150$  sec) and when the current switched from positive to negative ( $t=\pm 1740, \pm 4140$  and  $\pm 6540$  sec) or vice versa ( $t=\pm 1060, \pm 3460$  and  $\pm 5860$  sec). This last moment differed slightly for the different CV scans and the cycles within the scans.

### Preliminary Tests

Two preliminary tests were performed to further clarify the results found in this study. Firstly, different reactor parts were placed in tubes with fresh catholyte medium for five hours to measure whether these reactor parts would leach ions into the catholyte. For these leaching tests, the ion concentrations in the fresh medium were compared to those in the media with the reactor parts after five hours. The results can be found in SI Table 4. Secondly, a 50 ml sample with the highest optical density from biotic CV5 (day 224;  $t=1550$  sec) was centrifuged to measure which metallic compounds were present in the supernatant and which in the pellet. The supernatant was measured, and the pellet was measured separately after suspending in milliQ (SI Table 6).

### Analysis Methods

The metal concentrations in the catholyte and anolyte were analysed with an inductively coupled plasma analyzer (ICP-OES, Perkin Elmer AVIO 500). The used argon flow was 12 L/min. A multi-element standard solution was prepared in concentration ranges of 0–100 and 0–1000  $\mu\text{g/L}$ . The measured compounds included Fe, Cu, Ni, Mn, Zn, Co and Mo for the first four CV scans of the biotic experiments. For the fifth CV in the biotic system and the CV in the

abiotic systems, Ag, Al, Ba, Bi, Ca, Cd, Co, Cr, Cu, Fe, Ga, In, K, Li, Mg, Mn, Na, Ni, Pb, Sr, Zn, Mo, B, Tl, S and P were measured. The samples were acidified and pretreated by addition of 40  $\mu\text{l}$  65% HNO<sub>3</sub> and 40  $\mu\text{l}$  0.1 g/L Yttrium (internal standard) to 3920  $\mu\text{l}$  sample. Since a leakage occurred prior to CV5, the measurements of Fe, Co, Cu, Ni, Mn and Mo of CV5 were compared to those of CV2–4. No significant change in metal concentrations due to CV was found, so the metal measurements from CV5 are presented as well. ICP samples were also taken from the anolyte influent and effluent to verify whether metal species were exchanged with the anolyte. The OD<sub>600</sub> values of the reactor liquid were measured (Hach Lange DR 3900 Spectrophotometer) before and after the CV to monitor the change in suspended compounds due to the CV. The fatty acid productivities were measured with the same gas chromatography method as described by Jourdin, et al.<sup>[2c]</sup> The measurements of formic acid and lactic acid were performed with High Pressure Liquid Chromatography (HPLC, Ultimate 3000, Thermo Fisher Dionex). 20  $\mu\text{l}$  sample was loaded on an Aminex HPX-87H, 300x7.8 mm (Bio-Rad 125-0140) column at 35 °C. The flow rate was 0.5 ml/min and the mobile phase was 5 mM sulfuric acid.

In the experiments from this study acetate was found to be the only product. In the abiotic experiment no fatty acids or alcohols were formed (SI Table 1 and Table 2) and in the biotic experiment no fatty acids or alcohols were formed aside from acetate. No significant butyrate or ethanol productivity was observed during the continuous biotic CO<sub>2</sub> elongation experiment. Neither formate nor lactate were produced during the biotic and abiotic CVs, and the fatty acid concentrations did not measurably change during the scans.

### Contributor roles

SdS designed and performed the experiment, analysed, and interpreted data and drafted the manuscript. DS contributed to design and execution of the experiment, interpretation of the data, and revised the manuscript. HB contributed to experimental design, interpretation of the data and revising of the manuscript. CB contributed to experimental design and planning of the study and revised the manuscript. All authors read and approved the final manuscript.

### Funding information

This work was funded by a grant from the Wageningen Institute for Environment and Climate Research (WIMEK), and by the company ChainCraft B.V.

### Acknowledgements

Many thanks to Tomas van Haasterecht for the insightful discussions. Thanks to Kasper de Leeuw for manuscript revision.

### Conflict of Interest

The authors declare no conflict of interest.

**Keywords:** biocathode · bioelectrochemical synthesis · cyclic voltammetry · invasive · metal release

- [1] K. Rabaey, R. A. Rozendal, *Nat. Rev. Microbiol.* **2010**, *8*, 706–716.
- [2] a) A. A. Ragab, K. P. Katuri, M. Ali, P. E. Saikaly, *Front. Microbiol.* **2019**, *10*; b) N. Aryal, A. Halder, P.-L. Tremblay, Q. Chi, T. Zhang, *Electrochim. Acta* **2016**, *217*, 117–122; c) L. Jourdin, S. M. T. Raes, C. J. N. Buisman, D. P. B. T. B. Strik, *Front. Energy Res.* **2018**, *6*; d) I. Vassilev, P. A. Hernandez, P. Battle-Vilanova, S. Freguia, J. O. Krömer, J. R. Keller, P. Ledezma, B. Virdis, *ACS Sustainable Chem. Eng.* **2018**, *6*, 8485–8493; e) Z. Zaybak, B. E. Logan, J. M. Pisciotta, *Bioelectrochemistry* **2018**, *123*, 150–155; f) C. W. Marshall, D. E. Ross, E. B. Fichot, R. S. Norman, H. D. May, *Appl. Environ. Microbiol.* **2012**, *78*, 8412–8420; g) H. D. May, P. J. Evans, E. V. LaBelle, *Curr. Opin. Biotechnol.* **2016**, *42*, 225–233; h) V. Flexer, L. Jourdin, *Acc. Chem. Res.* **2020**, *53*, 311–321.
- [3] J. B. A. Arends, S. A. Patil, H. Roume, K. Rabaey, *J. CO<sub>2</sub> Util.* **2017**, *20*, 141–149.
- [4] S. M. T. Raes, L. Jourdin, C. J. N. Buisman, D. P. B. T. B. Strik, *ChemElectroChem* **2017**, *4*, 386–395.
- [5] N. Elgrishi, K. J. Rountree, B. D. McCarthy, E. S. Rountree, T. T. Eisenhart, J. L. Dempsey, *J. Chem. Educ.* **2017**, *95*, 197–206.
- [6] a) R. S. Nicholson, *Anal. Chem.* **1965**, *37*, 1351–1355; b) K. Yokoyama, Y. Kayanuma, *Anal. Chem.* **1998**, *70*, 3368–3376.
- [7] E. S. Rountree, B. D. McCarthy, T. T. Eisenhart, J. L. Dempsey, *ACS Publications* **2014**, *53*, 9983–10002.
- [8] a) D. Rand, R. Woods, *J. Electroanal. Chem.* **1972**, *36*, 57–69; b) A. D. Pozio, M. De Francesco, A. Cemmi, F. Cardellini, L. Giorgi, *J. Power Sources* **2002**, *105*, 13–19.
- [9] a) D. Grujicic, B. Pesic, *Electrochim. Acta* **2002**, *47*, 2901–2912; b) S. Rodrigues, A. Shukla, N. Munichandraiah, *J. Appl. Electrochem.* **1998**, *28*, 1235–1241; c) Y. Lai, F. Liu, Z. Zhang, J. Liu, Y. Li, S. Kuang, J. Li, Y. Liu, *Electrochim. Acta* **2009**, *54*, 3004–3010; d) J. Y. Lee, T. C. Tan, *J. Electrochem. Soc.* **1990**, *137*, 1402–1408.
- [10] F. Harnisch, S. Freguia, *Chemistry* **2012**, *7*, 466–475.
- [11] a) C. I. Torres, A. Kato Marcus, B. E. Rittmann, *Biotechnol. Bioeng.* **2008**, *100*, 872–881; b) A. De Lichtervelde, A. Ter Heijne, H. Hamelers, P. Biesheuvel, J. Dykstra, *Phys. Rev. Appl.* **2019**, *12*, 014018.
- [12] Z. Mao, Y. Sun, Y. Zhang, X. Ren, Z. Lin, S. Cheng, *Int. J. Hydrogen Energy* **2020**, *46(4)*, 3045–3055.
- [13] G. Pozo, L. Jourdin, Y. Lu, J. Keller, P. Ledezma, S. Freguia, *Electrochim. Acta* **2016**, *213*, 66–74.
- [14] a) K. Rabaey, N. Boon, S. D. Siciliano, M. Verhaege, W. Verstraete, *Appl. Environ. Microbiol.* **2004**, *70*, 5373–5382; b) H. S. Park, B. H. Kim, H. S. Kim, H. J. Kim, G. T. Kim, M. Kim, I. S. Chang, Y. K. Park, H. I. Chang, *Anaerobe* **2001**, *7*, 297–306; c) H. J. Kim, H. S. Park, M. S. Hyun, I. S. Chang, M. Kim, B. H. Kim, *Enzyme Microb. Technol.* **2002**, *30*, 145–152; d) E. Marsili, J. Sun, D. R. Bond, *Electroanalysis* **2010**, *22*, 865–874; e) S. M. Strycharz-Glaven, R. H. Glaven, Z. Wang, J. Zhou, G. J. Vora, L. M. Tender, *Appl. Environ. Microbiol.* **2013**, *79*, 3933–3942; f) D. Millo, *Biochem. Soc. Trans.* **2012**, *40*, 1284–1290.
- [15] K. Fricke, F. Harnisch, U. Schröder, *Energy Environ. Sci.* **2008**, *1*, 144–147.
- [16] J. Kang, T. Kim, Y. Tak, J.-H. Lee, J. Yoon, *J. Ind. Eng. Chem.* **2012**, *18*, 800–807.
- [17] a) E. Marsili, J. B. Rollefson, D. B. Baron, R. M. Hozalski, D. R. Bond, *Appl. Environ. Microbiol.* **2008**, *74*, 7329–7337; b) Y. Ruiz, J. A. Baeza, N. Montpart, J. Moral-Vico, M. Baeza, A. Guisasaola, *J. Chem. Technol. Biotechnol.* **2020**, *95*, 1533–1541.
- [18] K. de Leeuw, C. J. Buisman, D. P. Strik, *Environ. Sci. Technol.* **2019**, *53*, 7704–7713.
- [19] a) D. Grujicic, B. Pesic, *Electrochim. Acta* **2004**, *49*, 4719–4732; b) K. L. Hawthorne, T. J. Petek, M. A. Miller, J. S. Wainright, R. F. Savinell, *J. Electrochem. Soc.* **2014**, *162*, A108.
- [20] a) L. M. Huizar, C. Rios-Reyes, M. Rivera, *J. Chil. Chem. Soc.* **2017**, *62*, 3621–3626; b) K. Mishra, P. Singh, D. Muir, *J. Appl. Electrochem.* **2002**, *32*, 1391–1396.
- [21] Z. Zhou, Z. Pei, L. Wei, S. Zhao, X. Jian, Y. Chen, *Energy Environ. Sci.* **2020**, *13*, 3185–3206.
- [22] a) O. Choi, B.-I. Sang, *Biotechnol. Biofuels* **2016**, *9*, 11; b) S. W. Ragsdale, E. Pierce, *Biochim. Biophys. Acta Proteins Proteomics* **2008**, *1784*, 1873–1898.
- [23] a) L. Pang, M. Close, M. J. Noonan, M. Flintoft, P. Van den Brink, *J. Environ. Qual.* **2005**, *34*, 237–247; b) V. Bansal, A. Bharde, R. Ramanathan, S. K. Bhargava, *Adv. Colloid Interface Sci.* **2012**, *179–182*, 150–168.
- [24] T. H. Sleutels, *Microbial electrolysis kinetics and cell design* **2010**.
- [25] J. Palmer, S. Flint, J. Brooks, *J. Ind. Microbiol. Biotechnol.* **2007**, *34*, 577–588.
- [26] J. Barber, B. Conway, *J. Electroanal. Chem.* **1999**, *461*, 80–89.
- [27] S. Dai, P. Ravi, K. C. Tam, *Soft Matter* **2008**, *4*, 435–449.
- [28] A. W. Jeremiasse, H. V. Hamelers, C. J. Buisman, *Bioelectrochemistry* **2010**, *78*, 39–43.
- [29] M. Santini, S. Marzorati, S. Fest-Santini, S. Trasatti, P. Cristiani, *J. Power Sources* **2017**, *356*, 400–407.

Manuscript received: July 6, 2021

Revised manuscript received: August 10, 2021

Accepted manuscript online: August 19, 2021